

Induction of G₂/M phase arrest and apoptosis by potent antitumor APCA in human cervix carcinoma cells

Ke Xu, Xin Liang, Fang Wang, Lijuan Xie, Yufang Xu, Jianwen Liu and Xuhong Qian

3-(dimethylamino-ethylamino)-8-oxo-8H-acenaphthol[1, 2-b]pyrrole-9-carboxylic acid (APCA), as a potent antitumor compound, showed anticancer activity on a series of established cancer cells. Meanwhile, the cytotoxic effects of APCA were much smaller on normal human cells than that on cancer cells. This study investigated the molecular mechanisms underlying APCA-induced growth inhibition in HeLa cells. The results showed that the APCA-induced cell cycle arrest at G₂/M phase correlated with cyclinB1 and cyclin-dependent kinase 1 expression downregulation in a p53-independent manner, and also caused an increase in apoptosis, which was confirmed by characteristic morphological changes and increased apoptotic sub-G₁ population. Furthermore, translocation inhibition of nuclear factor- κ B, upregulation of Bax, and downregulation of Bcl-2, caspase-3 and caspase-9 activation, and poly-(ADP-ribose) polymerase cleavage were observed in HeLa cells treated with APCA, which indicated that the mitochondrial pathway was involved in the apoptosis signal pathway. In summary, APCA displayed an antitumor effect

through cell cycle arrest and apoptotic induction in HeLa cells, which suggested that APCA might have therapeutic potential against cervix carcinoma as an effective lead compound. *Anti-Cancer Drugs* 22:875–885 © 2011 Wolters Kluwer Health | Lippincott Williams & Wilkins.

Anti-Cancer Drugs 2011, 22:875–885

Keywords: antitumor, apoptosis, cell cycle arrest, G₂/M phase, HeLa human cervix carcinoma cells

State Key Laboratory of Bioreactor Engineering and Shanghai Key Laboratory of Chemical Biology, School of Pharmacy, East China University of Science and Technology, Shanghai, People's Republic of China

Correspondence to Dr Jianwen Liu and Xuhong Qian, State Key Laboratory of Bioreactor Engineering and Shanghai Key Laboratory of Chemical Biology, School of Pharmacy, East China University of Science and Technology, 268, 130 Meilong Road, Shanghai 200237, People's Republic of China
Tel/fax: +86 21 64252044;
e-mail: liujian@ecust.edu.cn; xhqian@ecust.edu.cn

Ke Xu and Xin Liang contributed equally to this study as joint first authors.

Received 3 March 2011 Revised form accepted 31 May 2011

Introduction

Cell cycle control is the major regulatory mechanism in the cell growth process [1]. Many cytotoxic agents and/or DNA-damaging agents arrest the cell cycle at the G₀/G₁, S, or G₂/M phase and then induce apoptosis [2]. Several studies have shown that various cytotoxic drugs can induce G₂/M phase accumulation [3]. G₂ to M phase progression is regulated by a number of the cyclin/cyclin-dependent kinase 1 (Cdk) family; in particular, activation of the cyclinB1/Cdk1 complex is required for transition from G₂ to the M phase [4]. In addition to the cell cycle, several therapeutic and chemopreventive agents eliminate cancerous cells by inducing apoptosis. Apoptosis is an intracellular suicide program that is executed by the activation of caspases, a family of cytoplasmic cysteine proteases [5]. Caspase-3, caspase-8, and caspase-9, as key components of the apoptotic machinery, have been shown to be activated in apoptotic cells and cleave several cellular proteins including poly-(ADP-ribose) polymerase (PARP) protein, the cleavage of which is a hallmark of apoptosis.

3-(Dimethylamino-ethylamino)-8-oxo-8H-acenaphthol [1, 2-b]pyrrole-9-carboxylic acid (APCA), which was synthesized in our laboratory, exhibited cytotoxic activity in a series of human tumor cell lines, of which HeLa human cervix carcinoma cells were the most sensitive ones. It was revealed that APCA markedly inhibited HeLa

cell growth with a 50% cell growth inhibition (IC₅₀) of 30 μ mol/l. Therefore, this new investigation will be helpful in further elucidation of undiscovered biological properties of this novel antitumor agent to HeLa cells.

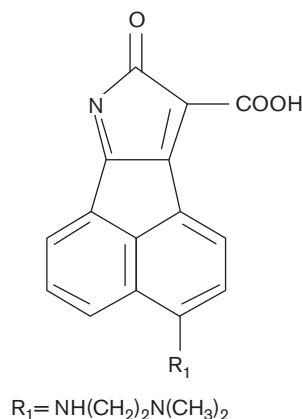
The development of a new, active anticancer agent raises important questions about its mechanism of action. In this study, we assessed the antitumor activity of APCA in a series of established cancer cell lines by 3-(4,5-dimethylthiazol-2-yl)-2,5-diphenyltetrazolium bromide (MTT) assay and colony-forming assay, among which the cervix carcinoma HeLa cell line was the most sensitive. Then, we further studied the antiproliferation effects of APCA on HeLa cells. We found that APCA can present antitumor effects by inducing G₂/M phase arrest and apoptosis, and then we looked into the mechanism. Here, we provide evidence that APCA induced G₂/M arrest and subsequent apoptosis in HeLa human cervix carcinoma cells.

Materials and methods

Drug and materials

APCA was synthesized in our laboratory by Xie Lijuan (Fig. 1) [6]. The compound was dissolved in dimethyl sulfoxide. The control cells were treated with the same amount of vehicle alone. The final DMSO concentration never exceeded 0.1% (v/v), in either control or treated samples. Roswell Park Memorial Institute (RPMI) 1640

Fig. 1



Structure of 3-(dimethylamino-ethylamino)-8-oxo-8H-acenaphthol [1,2-b]pyrrole-9-carboxylic acid (APCA).

medium, Dulbecco's modified Eagle's medium, fetal calf serum, trypan blue, penicillin G, and streptomycin were obtained from Gibco BRL (Gaithersburg, Maryland, USA).

MTT, DMSO, ribonuclease, Hoechst 33258, propidium iodide, and 5-bromo-4-chloro-3-indolyl-phosphate (BCIP)/nitro blue tetrazolium were purchased from Sigma Chemical (St Louis, Missouri, USA); human reactive monoclonal antibodies against cyclinB1, Cdk1, p53, p21, nuclear factor κB (NF- κB), Bcl-2, Bax, cleaved PARP, and β -actin were purchased from Santa Cruz Biotechnology (Santa Cruz, California, USA), and antimouse and antirabbit IgG peroxidase-conjugated secondary antibody were purchased from Pierce (Rockford, Illinois, USA).

Cell lines and cell culture

The human cell lines used included human cervix carcinoma cells, HeLa; human cervical carcinoma cells, SiHa; human cervix epithelioid carcinoma cells, HeLa299; human leukemia cells, HL-60; human breast cancer cells, MCF-7; human late-stage hormone-insensitive breast cancer cells, MDA-MB-231; human malignant melanoma cells, A375; human colon cancer cells, HCT-8; embryonic kidney cells, HEK293; and embryonic liver cells, L-02. All cells were purchased from Cell Bank of Type Culture Collection of Chinese Academy of Sciences (Shanghai, China). HeLa, SiHa, HeLa299, HL-60, and HCT-8 cells were cultured in RPMI 1640 medium supplemented with 10% heat-inactivated bovine serum, penicillin (100 U/ml), and streptomycin (100 U/ml). MCF-7 and MDA-MB-231 cells were cultured in RPMI 1640 medium supplemented with 15% heat-inactivated fetal bovine serum, penicillin (100 U/ml), and streptomycin (100 U/ml). A375 cells were cultured in Dulbecco's modified Eagle's medium with 10% heat-inactivated bovine serum, penicillin (100 U/ml), and streptomycin (100 U/ml). HEK293 and L-02 cells were cultured in RPMI 1640 medium, supplemented with 10% heat-inactivated fetal calf serum,

penicillin (100 U/ml), and streptomycin (100 U/ml). Cells were incubated at 37°C in a humidified atmosphere of 95% air and 5% CO_2 .

Analysis of cytotoxicity

The cytotoxicity assay was determined by MTT assay [7] and the trypan blue dye exclusion assay was performed to confirm and verify cell viability. HeLa, SiHa, HeLa299, HL-60, MCF-7, MDA-MB-231, A375, HCT-8, HEK293, and L-02 cells were seeded at a density of 1×10^4 cells/well in 100 μl of the cell culture medium in 96-well culture plates. After 12 h incubation, the cells were treated with APCA from 0 to 150 $\mu\text{mol/l}$ in medium for 24 h. Then, MTT solution (5 mg/ml) was added to each well and incubated at 37°C for 4 h. Then, supernatants were removed and replaced by 100 μl of DMSO. The optical density in control and drug-treated wells was measured in an Automated Microplate Reader (Multiskan Ex, Lab systems, Finland) at a test wavelength of 570 nm. The cytotoxicity of APCA was expressed as IC_{50} (concentration of 50% cytotoxicity, which was extrapolated from linear regression analysis of experimental data).

Colony-forming (clonogenic) assay

HeLa, SiHa, HeLa299, HL-60, MCF-7, MDA-MB-231, A375, and HCT-8 cells were seeded in 24-well culture plates (200–300 cells/well) respectively, and allowed to adhere for 12 h before treatment. Culture medium containing increasing drug concentrations was added to cells, followed by incubation for 7 days in the presence of drug. After this time, cells were then rinsed with phosphate buffered saline (PBS), fixed with methanol, and stained with 0.2% crystal violet solution, and colonies (> 50 cells) were counted [8]. The antiproliferative activity was expressed as inhibiting concentration 50% (EC_{50}).

Fluorescent morphological assay [9]

Cells from exponentially growing cultures were seeded in 24-well culture plates and treated with APCA (30 $\mu\text{mol/l}$) for 24 or 48 h. Cells were washed with PBS, fixed in MeOH-HAc (3:1, v/v) for 10 min at 4°C, stained with Hoechst 33258 (5 $\mu\text{g/ml}$ in PBS) for 5 min at room temperature, and then examined by using a LEICA DMIRB fluorescence microscope (Leica, Wetzlar, Germany) at 356 nm.

Flow cytometric analysis of cellular DNA content

Flow cytometric analysis of cellular DNA content was carried out as described previously [10]. Cells (2×10^5) were seeded in a six-well culture plate; after 12 h incubation, cells were treated with 0, 7.5, 15, and 30 $\mu\text{mol/l}$ of APCA for 0, 12, 24, 36, and 48 h, respectively. Both floating and attached cells were collected by trypsinase and poured together into the centrifuge tubes. Cells were washed with PBS, resuspended, and fixed in 70% ice-cold ethanol for 4 h at 4°C. Subsequently, they were treated with ribonuclease A (50 $\mu\text{g/ml}$) for 30 min. Finally, cells

were stained with propidium iodide (50 µg/ml) and analyzed in an FACScan flow cytometer (Becton Dickinson, USA). The percentage of cells in G₀/G₁ phase, S phase, G₂/M phase, and sub-G₁ phase was analyzed using standard ModFit and CellQuest software programs (San Jose, California, USA).

Assays of caspase activity

Cells (1×10^6 /dish) were seeded in 10-cm dishes. After 12 h incubation, cells were treated with 0, 7.5, 15, and 30 µmol/l of APCA for 48 h. After treatment, both floating and attached cells were collected by trypsinase and washed three times with PBS and resuspended in Tris-HCl (50 mmol/l, pH 7.4), EDTA (1 mmol/l), and ethyleneglycoltetraacetic acid (10 mmol/l). Cell lysates were clarified by centrifugation at 18 000 g for 3 min, and clear lysates containing 50 µg of protein were incubated with enzyme-specific colorigenic substrates (100 µmol/l) at 37°C for 1 h. The activity of caspase-3, caspase-8, and caspase-9 was described as the cleavage of colorimetric substrate by measuring the absorbance at 405 nm.

Western blotting analysis

Cells (1×10^6 /dish) were seeded in 10-cm dishes. After 12 h incubation, cells were treated with 0, 7.5, 15, and 30 µmol/l of APCA for 24 and 48 h, respectively. For total cell protein extracts, control and treated cells were washed in PBS, suspended in lysis buffer containing Tris-HCl (50 mmol/l pH 7.5), 1% NP-40, EDTA (2 mmol/l), NaCl (10 mmol/l), aprotinin (10 µg/ml), leupeptin (10 µg/ml), dithiothreitol (1 mmol/l), 0.1% SDS, and phenylmethylsulfonyl fluoride (1 mmol/l) and placed in ice for 30 min. After centrifugation for 15 min at 4°C, the supernatant was collected. Extraction and isolation of nuclear fraction were performed according to the method of Levites *et al.* [11]. Protein concentrations were determined using the BCA assay (Pierce).

The western blotting assay was performed as described previously [12]. For western blotting analysis, equal amount of proteins (30 µg) were separated by SDS-polyacrylamide gel electrophoresis and transferred to a nitrocellulose membrane. The blotting was blocked in blocking buffer (5% nonfat dry milk/0.1% Tween 20 in PBS) for 1 h at room temperature, and then incubated with appropriate primary antibodies in blocking buffer overnight at 4°C. The blotting was then incubated with appropriate secondary antibody alkaline phosphatase conjugated and detected in 5 ml of alkaline phosphatase buffer containing 16.5 µl of BCIP and 33 µl of nitro blue tetrazolium at room temperature for 10–20 min, and then photographed. Beta-actin was used as a loading control.

Semiquantitative RT-PCR analysis

Total RNA of APCA-treated cells was extracted using TRIzol reagent (Promega Corporation, Madison, Wisconsin, USA) according to the supplier's instruction. RNA was

quantified by optical density measurement at 260 and 280 nm using a spectrophotometer (all RNA samples had an A₂₆₀/A₂₈₀ ratio >1.8), and integrity was confirmed by running RNA on a 1.2% agarose gel. Then, RNA was reverse-transcribed using a Reverse Transcription System (Takara Shuzo, Shiga, Japan). Primers were obtained from Shanghai Sangon Biological Engineering Technology and Services Co., Ltd. (Shanghai, China) and their sequences were: 5'-GGTCGGAGTCAACGGATTG-3' (sense) and 5'-ATGAGCCCCAGCCTTCTCAT-3' (antisense) for glyceraldehyde-3-phosphate dehydrogenase, 5'-CTTATACTAAGCACCAAATC-3' (sense) and 5'-CTTGGCTAAATCTTGAAC-3' (antisense) for cyclinB1, 5'-CTTATGCAGGATTCCAGGTT-3' (sense) and 5'-GGTGCCTATACTCCAAATGTC-3' (antisense) for Cdk1, 5'-AGATTGCCCTCTCAGTGTCCA-3' (sense) and 5'-TGGAAGGAAGAAAAGCTGCC-3' (antisense) for CDK4, 5'-AAGCTGTGCATCTACACCGA-3' (sense) and 5'-CTTGAGCTTGTTCCACCAGGA-3' (antisense) for cyclin D1, 5'-GTTCCGAGAGCTGAATGAGG-3' (sense) and 5'-TGAGTCAGGCCCTTCTGTCT-3' (antisense) for p53, 5'-CGCGACTGTGATGCGCTA-3' (sense) and 5'-AAGTCGAAGTTCCATCGCTCA-3' (antisense) for p21. An aliquot (2 µl) of reverse transcription (RT) product was used for PCR amplification in a total volume of 25 µl. Amplification of Cdk1, cyclinB1, cyclin D1, CDK4, p53, and p21 using a BADRED thermal cycler (Foster, California, USA) consisted of 30 cycles (95°C for 30 s, 54°C for 30 s, 72°C for 30 s for cyclin B1 and Cdk1; 95°C for 30 s, 55°C for 30 s, 72°C for 30 s for p53, p21, cyclin D1, and CDK4), whereas glyceraldehyde-3-phosphate dehydrogenase was used as a control for 30 cycles (94°C for 30 s, 55°C for 30 s, and 72°C for 30 s). The PCR conditions were optimized to keep the amplification in the linear range to avoid the plateau effect. The amplified DNA was analyzed on a 1.5% agarose gel and photographed. Densitometric analysis of the images was carried out with image analysis software (Image Gauge 3.0.1, Fuji Photo Film, Tokyo, Japan). Results were presented as normalized fold changes in relation to control.

Statistical analysis

All data were expressed as mean ± standard deviation. Statistical analysis was carried out using the Origin7.0 software (OriginLab Corp., Northampton, Massachusetts, USA) to evaluate the significance of differences between groups considered as **P* < 0.05; ***P* < 0.01; ****P* < 0.001. All data points represented the mean of triplicates.

Results

Cytotoxicity effect of APCA in eight human cancer cell lines

The cytotoxicity of APCA on various cells was shown in Fig. 2. The data indicated that cytotoxicity of APCA on all cell lines was dose-dependent and each cell had a different sensitivity to the inhibitive effect of the APCA (Fig. 2a). The IC₅₀ values, cytotoxicity, EC₅₀, and

therapeutic index (IC_{50} vs. EC_{50}) are shown in Table 1. The proliferation of HeLa cells was reduced by 50% upon an APCA (30 $\mu\text{mol/l}$) exposure for 24 h, which is the dose referred in the following experiments. In addition, we also chose 0, 7.5, and 15 $\mu\text{mol/l}$ in the following experiments. At these concentrations, the drug had less toxic effect on HEK293 and L-02 (Fig. 2b).

Effect of APCA on colony formation of eight human cancer cell lines

The EC_{50} values on colony formation are shown in Table 1. On counting the above-mentioned results, the therapeutic index (the ratio of IC_{50} vs. EC_{50}) for

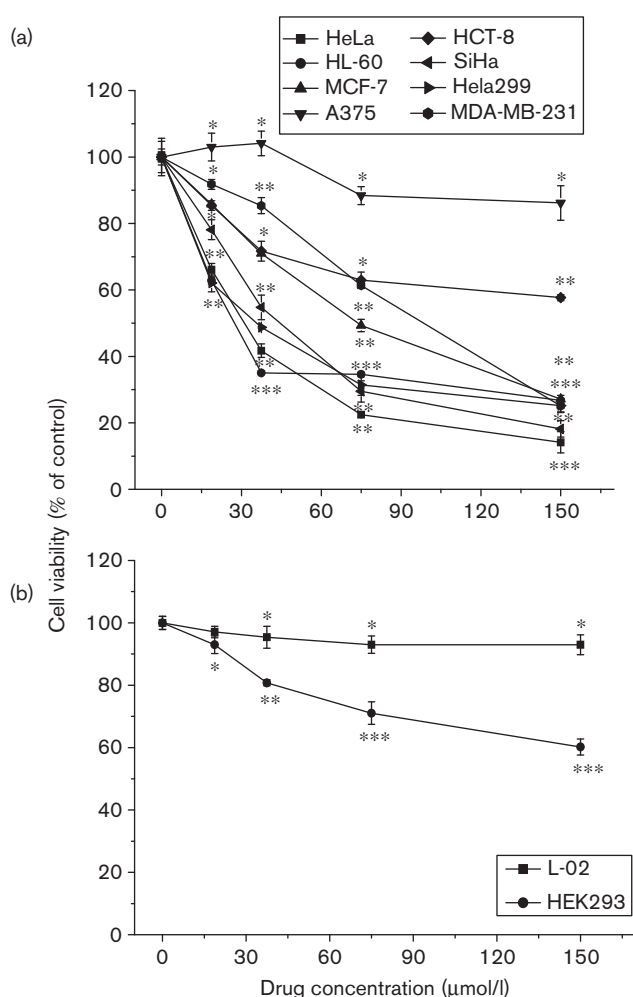
Table 1 Growth inhibition effect of APCA on five established cancer cell lines^a

	HeLa	SiHa	HeLa299	HL-60
IC_{50} ($\mu\text{mol/l}$)	29.3 \pm 2.12	44.38 \pm 3.62	35.11 \pm 2.12	27.1 \pm 1.2
EC_{50} ($\mu\text{mol/l}$)	1.94 \pm 0.5	5.13 \pm 0.82	3.33 \pm 0.76	5.6 \pm 0.7
TI	15.1	8.65	10.54	4.84
	MCF-7	MDA-MB-231	A375	HCT-8
IC_{50} ($\mu\text{mol/l}$)	70.5 \pm 5.13	98.45 \pm 6.73	> 150	> 150
EC_{50} ($\mu\text{mol/l}$)	16 \pm 1.4	21.5 \pm 2.97	NA	NA
TI	4.41	3.13	NA	NA

APCA, 3-(dimethylamino-ethylamino)-8-oxo-8H-acenaphthol [1,2-b] pyrrole-9-carboxylic acid; EC_{50} , 50% cell growth inhibition; IC_{50} , 50% cell growth inhibition; NA, not applicable; TI, therapeutic index.

^aEach value represented mean \pm standard deviation of three independent experiments. TI was equal to the ratio of IC_{50} vs. EC_{50} .

Fig. 2



Effect of 3-(dimethylamino-ethylamino)-8-oxo-8H-acenaphthol [1,2-b] pyrrole-9-carboxylic acid on the viability of (a) HeLa, HL-60, MCF-7, A375, HCT-8, SiHa, HeLa299, and MDA-MB-231 cells, or (b) L-02 and HEK293 cells. Cells were treated for 24 h in the presence of 3-(dimethylamino-ethylamino)-8-oxo-8H-acenaphthol [1,2-b] pyrrole-9-carboxylic acid in medium. Cell viability was then determined by an 3-(4,5-dimethylthiazol-2-yl)-2,5-diphenyltetrazolium bromide assay and was expressed as mean \pm standard deviation of three separate experiments. Significant differences from untreated control are indicated by * P <0.05; ** P <0.01; *** P <0.001.

these eight human cancer cell lines showed the following order: HeLa > HeLa299 > SiHa > HL-60 > MCF-7 > MDA-MB-231 > A375, HCT-8 successively. It showed that HeLa cells, which were referred to in the following experiments, were most sensitive to APCA with a therapeutic index equal to 15.1.

Time-dependent and dose-dependent effects of APCA on HeLa cells

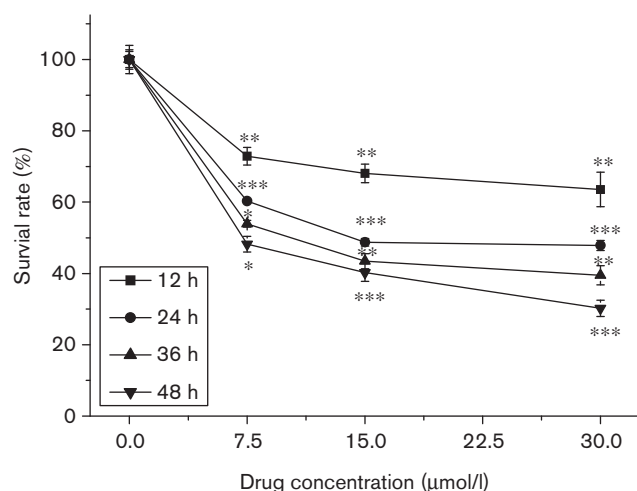
To further evaluate the antiproliferation effect of APCA on HeLa cells, we initially treated cells with APCA for 12, 24, 36, and 48 h, respectively. Cell viability was estimated by the MTT assay. Figure 3 demonstrated that APCA inhibited cellular proliferation in a time-dependent and dose-dependent manner.

Effect of APCA on the cell morphology

The growth-inhibitory effect of APCA was accompanied by cell shrinkage as observed (Fig. 4), which might indicate apoptosis. We further examined the morphological changes in response to APCA treatment by fluorescence staining. Both control and APCA-treated cells were stained with the fluorescence dye Hoechst 33258 and visualized using a fluorescence microscope. The control cells were normal and the nuclei were round and homogeneous, whereas the cells treated with APCA exhibited the characteristics of apoptosis, with cell shrinkage, nuclear condensation, and fragmentation in a time-dependent manner (Fig. 4).

Effect of APCA on G_2/M phase arrest

To determine whether a decrease in cell viability involved cell cycle changes, we investigated the effect of APCA on cell cycle distribution by flow cytometry. An exposure of cells to 0, 7.5, 15, and 30 $\mu\text{mol/l}$ APCA for 24 h resulted in the accumulation of G_2/M phase, from 12.86 to 16.53%, 20.98, and 35.41%, respectively (Fig. 5). APCA can cause a time-dependent G_2/M phase arrest, and G_2/M phase accumulation peaked when cells were treated with APCA (30 $\mu\text{mol/l}$) for 24 h (Fig. 6a and b). These results suggested that APCA inhibited the cellular proliferation by G_2/M phase arrest in a time-dependent and dose-dependent manner.

Fig. 3

Dose and time effect of 3-(dimethylamino-ethylamino)-8-oxo-8H-acenaphthol [1,2-b] pyrrole-9-carboxylic acid on the viability of HeLa cells. Cells were treated for 12, 24, 36, and 48 h in the presence of 3-(dimethylamino-ethylamino)-8-oxo-8H-acenaphthol [1,2-b] pyrrole-9-carboxylic acid in medium. Cell viability was then determined by an 3-(4,5-dimethylthiazol-2-yl)-2,5-diphenyltetrazolium bromide assay and expressed as mean \pm standard deviation of three separate experiments. Significant differences from control are indicated by * P <0.05; ** P <0.01; *** P <0.001.

Effect of APCA on apoptosis

We also quantified the cells in the sub-G₁ population after APCA treatment as the apoptosis index. Cells treated with 30 μmol/l of APCA for escalating time resulted in an obvious increase of the sub-G₁ fraction (especially treatment for more than 24 h), which increased from 0 to 12.22% (36 h) and 14.17% (48 h) in a time-dependent manner (Fig. 6c).

Effects of APCA on caspase activation

To further characterize the apoptotic pathway activated by APCA, we determined the kinetics of caspase activation. The activation of caspases in APCA-treated cells was assessed using colorigenic tetrapeptide substrates, Ac-IETD-pNA, Ac-LEHD-pNA, and Ac-DEVD-pNA, which have been shown to be selective for caspase-8, caspase-9, and caspase-3-like enzymatic activities, respectively. Treatment of HeLa cells with 0, 7.5, 15, and 30 μmol/l APCA results in the detection of caspase-9 and caspase-3 activation at 48 h (Fig. 7). Results demonstrated that APCA-induced apoptosis are significant. These results confirm involvement of caspase-3 and caspase-9 in APCA-mediated cell death.

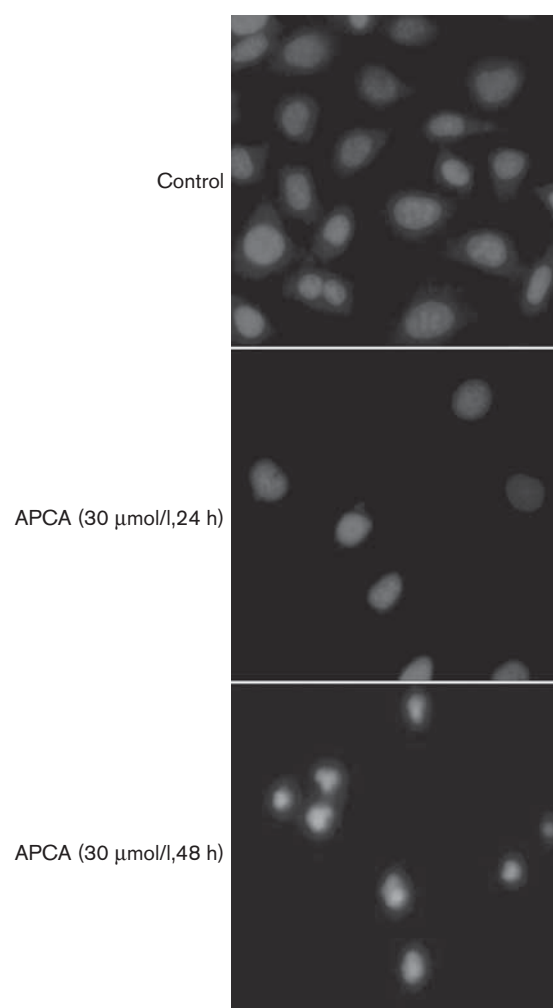
Effect of APCA on Cdk1 and cyclinB1 expression

In an attempt to understand the effect of the molecular events involved in APCA activity on cell cycle progression, we next investigated the effect of the APCA on the expression of proteins that were pivotal for G₂/M transition, including Cdk1 and cyclinB1. G₂/M transition requires activity of cyclin-dependent kinase, Cdk1,

which was positively regulated by association with cyclinB1. Figure 8a represented a western blotting result from treated (7.5, 15, and 30 μmol/l APCA) and untreated cells, and a decrease in the level of cyclinB1 and Cdk1 protein was observed at 24 h posttreatment, which suggested that downregulation of the expression of G₂ phase regulating proteins might contribute to APCA-mediated cell cycle arrest in HeLa cells.

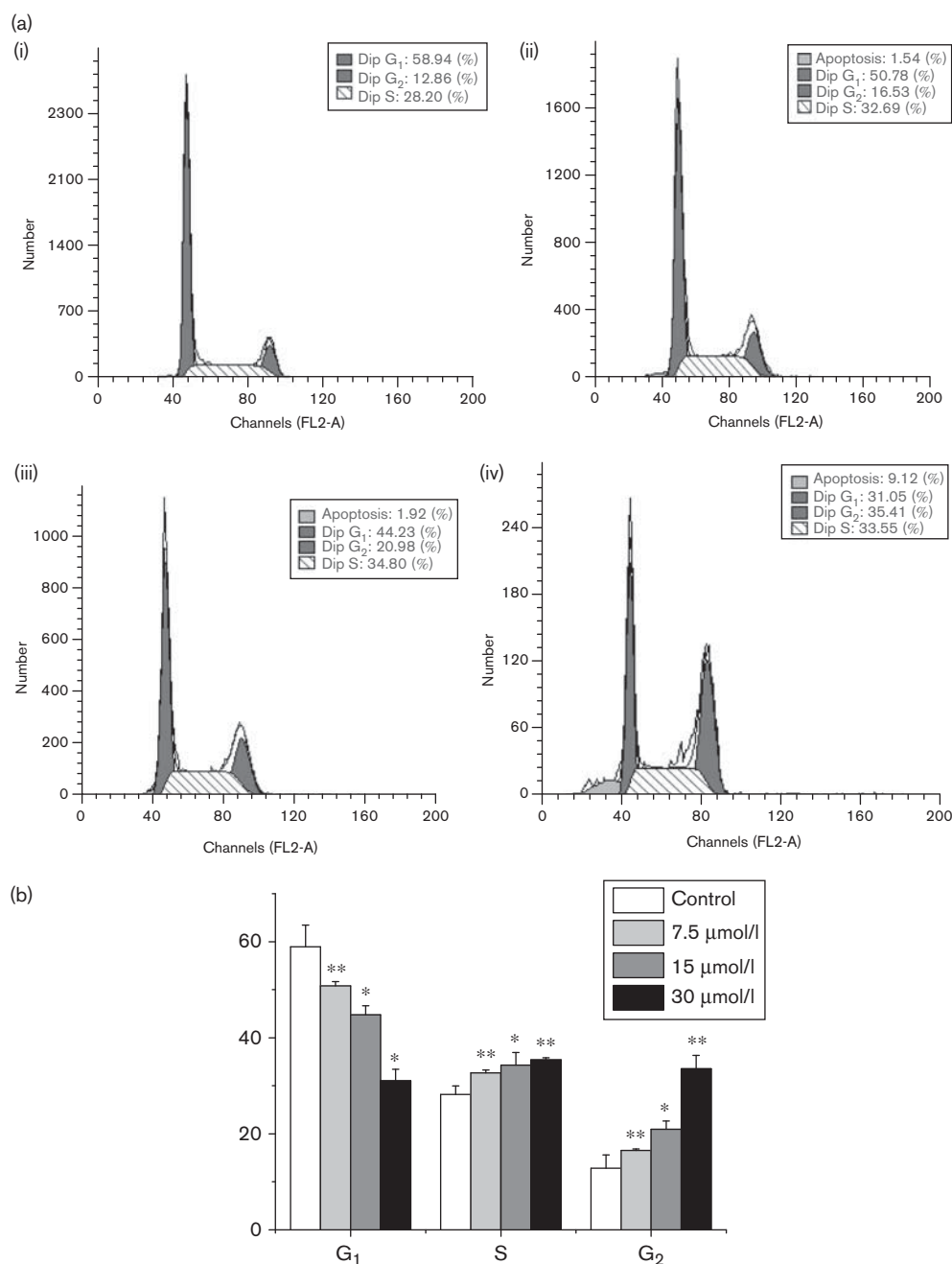
Effect of APCA on p53 and p21 expressions

To further investigate molecular changes involved in APCA-mediated G₂/M cell cycle arrest in HeLa cells, we also analyzed the expression of p53 and p21 by western blotting. The tumor suppressor gene, p53, is known to be a member

Fig. 4

Fluorescent staining of nuclei in 3-(dimethylamino-ethylamino)-8-oxo-8H-acenaphthol [1,2-b] pyrrole-9-carboxylic acid (APCA)-treated and untreated cells by Hoechst 33258. HeLa cells were treated with APCA (30 μmol/l) for 24 or 48 h. Cells untreated and cells treated with APCA were visualized using a LEICA fluorescence microscope. Condensed and fragmented nuclei and apoptotic bodies (arrows) were seen in the APCA-treated cells, but not in the control.

Fig. 5

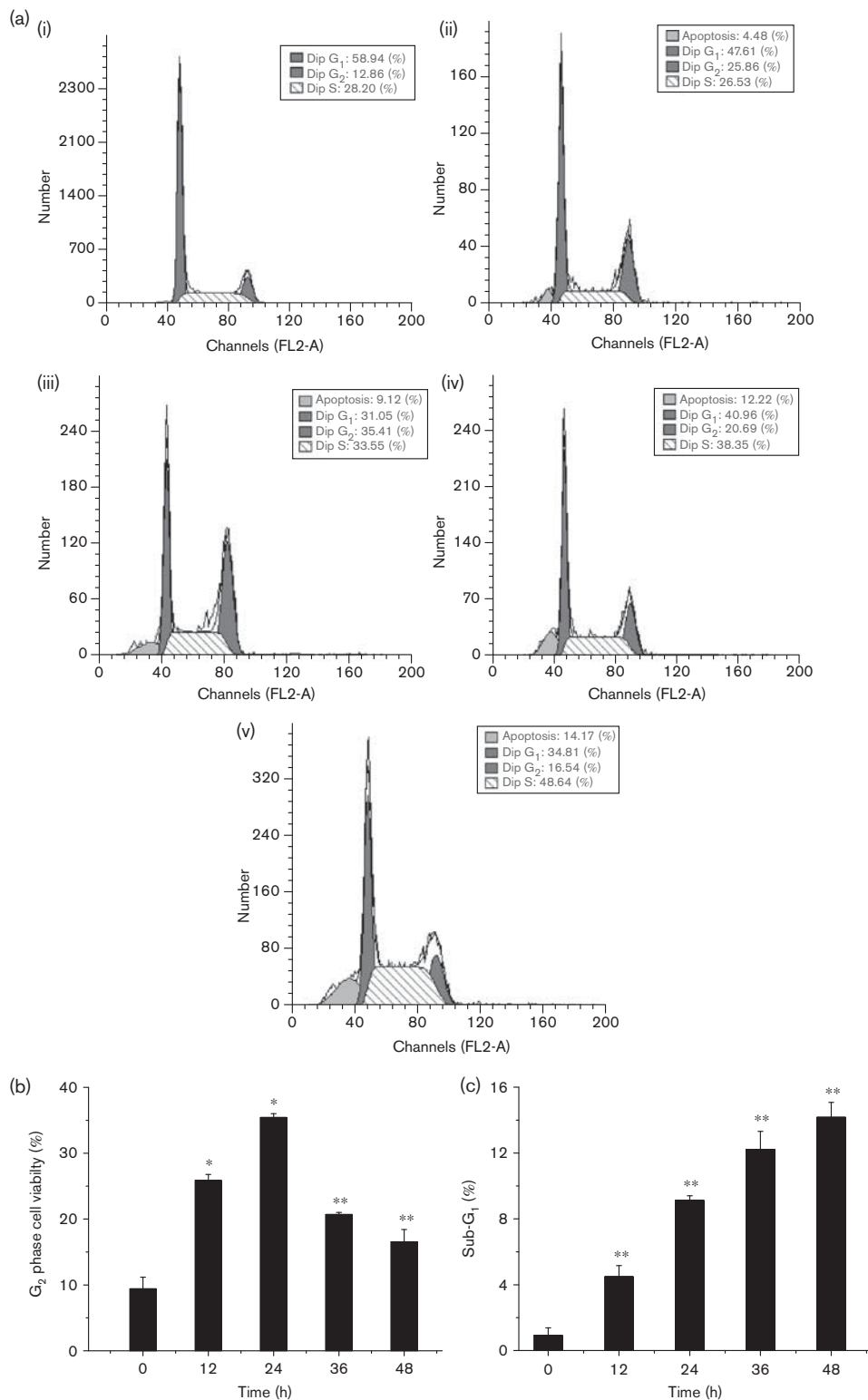


Dose-dependent effect of 3-(dimethylamino-ethylamino)-8-oxo-8H-acenaphthol [1,2-*b*] pyrrole-9-carboxylic acid (APCA) on cell cycle distribution. (a) HeLa cells were treated with different concentrations of APCA and analyzed at 24 h by DNA flow cytometry. (i) Control, (ii) 7.5 μmol/l APCA, (iii) 15 μmol/l APCA, and (iv) 30 μmol/l APCA. (b) Histograms showed number of cells per channel (vertical axis) vs. DNA content (horizontal axis). The values indicated the percentage of cells in the indicated phases of the cell cycle. The data shown are representative of three independent experiments with similar findings. Significant differences from control are indicated by * $P < 0.05$; ** $P < 0.01$.

of the DNA damage-response pathway. It has been proved that p53 protein increases at the early stages of cellular damage in response to a variety of stress-inducing agents [13], being responsible for the inhibition of cell growth and/or commitment to apoptosis. p53 protein was analyzed by western blotting after treatments with 0, 7.5,

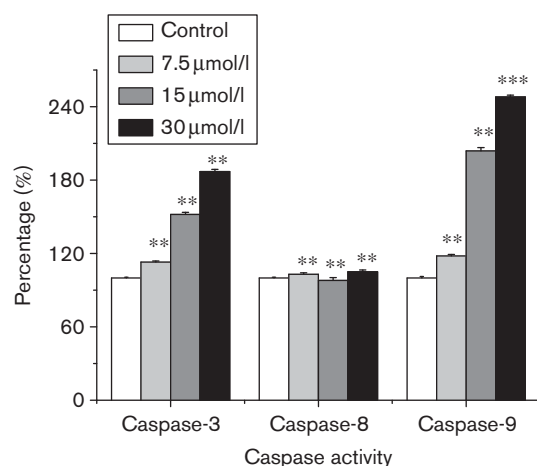
15, and 30 μmol/l APCA (Fig. 8b), which showed that APCA induced no obvious change of p53. Meanwhile, we analyzed the expression of its downstream effector p21, a potent inhibitor of cell cycle kinases. In fact, the p21 protein level also had no obvious change, indicating that APCA had no significant effect on the p53/p21 system.

Fig. 6



Time-dependent effect of 3-(dimethylamino-ethylamino)-8-oxo-8H-acenaphthol [1,2-*b*] pyrrole-9-carboxylic acid (APCA) on a population of G₂ phase cells and hypodiploid cells. (a) HeLa cells treated with APCA (30 μmol/l) for 12, 24, 36, and 48 h and analyzed by DNA flow cytometry. (i) Control, (ii) 12 h, (iii) 24 h, (iv) 36 h, (v) and 48 h. (b) The percentage of G₂ phase cells showed a time-dependent response to APCA. G₂ phase accumulation peaked at 24 h treatment. (c) The percentage of sub-G₁ cells showed a time-dependent response to APCA. Data are expressed as mean ± standard deviation of three separate experiments. Significant differences from control are indicated by **P* < 0.05; ***P* < 0.01.

Fig. 7



Effects of 3-(dimethylamino-ethylamino)-8-oxo-8H-acenaphthol [1,2-b] pyrrole-9-carboxylic acid (APCA) on caspase-3, caspase-8, and caspase-9 activations. Activation of caspase-3 and caspase-9 by APCA. After treatment with 0, 7.5, 15, and 30 μmol/l of APCA for 48 h, cell lysates were prepared and enzymatic activity of caspase-3, caspase-8, and caspase-9 proteases was determined as described under Materials and methods section. Significant differences from the control are indicated by ** $P < 0.01$; *** $P < 0.001$.

Effect of APCA on cell nuclear translocation of NF-κB, the expression of Bcl-2 and Bax

To understand the effect of the molecular events involved in APCA activity on cell apoptosis, we next investigated the effect of the APCA on the expression and nuclear translocation of NF-κB, and the expression of proteins that were pivotal for apoptosis, including Bcl-2 and Bax. The result showed that nuclear translocation of NF-κB reduced, but no obvious changes were found in its expression (Fig. 8c). Meanwhile, upregulation of Bax and downregulation of Bcl-2 were observed, suggesting that an increase in Bax/Bcl-2 ratios might be involved in apoptosis induced by APCA (Fig. 8d).

Effect of APCA on PARP cleavage

We also examined PARP proteolysis as a marker of caspase activation. PARP is a highly conserved nuclear enzyme involved in DNA repair and activated in response to DNA damage [14,15]. It is also a preferential substrate for caspase-3, which is cleaved by this protein into 89-kDa and 24-kDa fragments during apoptosis. Figure 8d showed PARP cleavage in cells treated with APCA for up to 48 h. APCA was very efficient in inducing PARP cleavage, as reflected by the intensity of the 89 kDa PARP fragments, which were clearly visible after 48 h of incubation with the drug.

Effect of APCA on mRNA levels of cell cycle genes

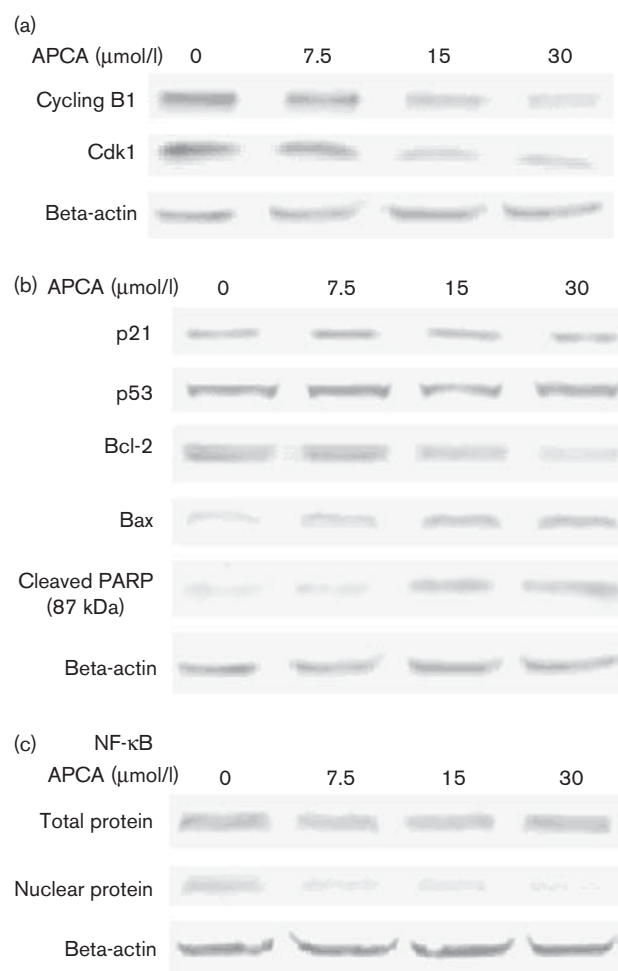
We had determined that APCA could induce G_2/M phase arrest, and then we examined the mRNA levels of cell cycle genes by semiquantitative RT-PCR analysis. The results indicated that the mRNA expression of cyclinB1

and Cdk1 decreased after APCA treatment in a dose-dependent manner, and no obvious change in the mRNA expression of cyclin D1, CDK4, p53, and p21 was observed (Fig. 9). Thus, APCA decreased the expression of cyclinB1 and Cdk1 at transcription level.

Discussion

Many anticancer agents and DNA-damaging agents arrest the cell cycle at the G_0/G_1 , S, or G_2/M phase and then induce apoptosis [16]. Cell cycle checkpoints may function to ensure that cells have time for DNA repair,

Fig. 8



Western blotting analysis of protein extracts obtained from HeLa cells treated with 0, 7.5, 15, and 30 μmol/l 3-(dimethylamino-ethylamino)-8-oxo-8H-acenaphthol [1,2-b] pyrrole-9-carboxylic acid (APCA), respectively. (a) Total protein extracts were prepared after treatment for 24 h, and then analyzed by western blotting with antibodies to cyclin-dependent kinase 1 (Cdk1) and cyclin B1. (b) Total protein extracts were prepared after treatment for 24 h, and analyzed with antibodies to p53, p21, Bcl-2, Bax, and cleaved poly-(ADP-ribose) polymerase (PARP). (c) Total protein and nuclear extracts were prepared after treatment for 24 h, respectively, and analyzed with antibodies to nuclear factor-κB (NF-κB) (p65 subunit). Beta-actin was used as a loading control. Western blotting were representative of three independent experiments.

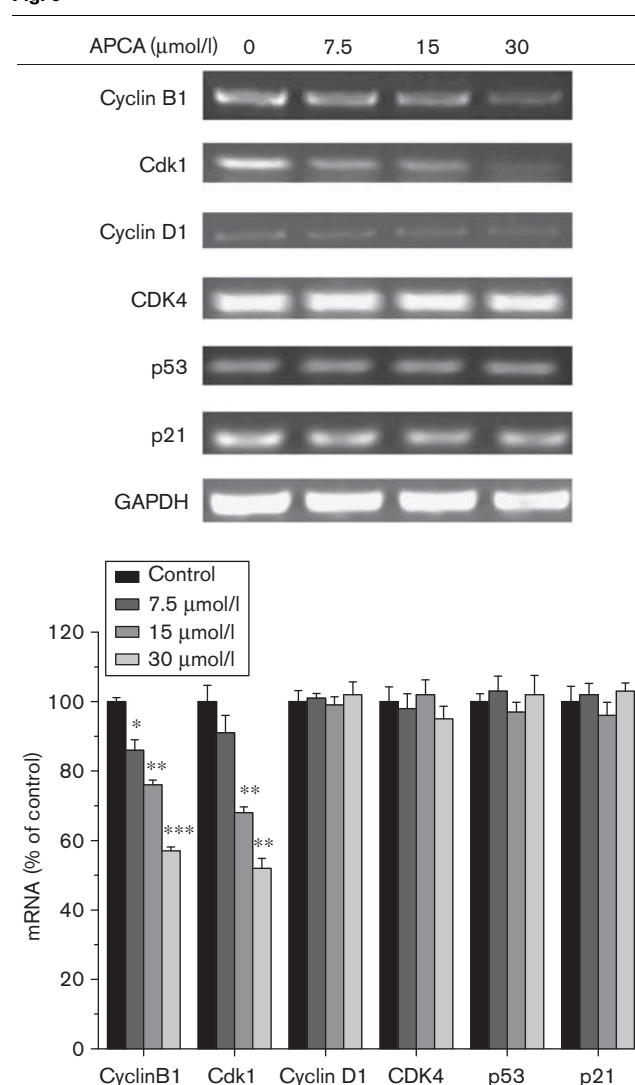
whereas apoptosis may function to eliminate irreparable or unrepaired damaged cells. The purpose of this study was to evaluate cytotoxicity of APCA on human cancer lines in comparison with noncancerous human cells; as the HeLa cell line was the most sensitive cell line to treatment according to therapeutic index, which indicated that APCA may be an effective lead compound against cervix carcinoma (Table 1), further investigations were performed to elucidate the molecular mechanism of action by which APCA inhibited cell viability of HeLa cells. APCA had a time-dependent and dose-dependent cytotoxic effect on HeLa cells. As shown in Figs 5 and 6, APCA induced cell cycle arrest in the G₂/M phase and apoptosis in HeLa cells. G₂/M phase accumulation and apoptosis have been observed in cells exposed to DNA-damaging agents such as γ -irradiation [17], microtubule-stabilizing agents [18], and topoisomerase inhibitors [19]. Current studies involved in developing effective cancer preventive approaches have focused mainly on the use of natural bioactive agents that can induce selective cytotoxicity in cancer cells [20]. Hence, we examined the cytotoxicity in HEK293 cells and L-02 cells. By comparison, we found that the cytotoxicity of APCA on cancer cells was much stronger than that on noncancerous cells (Fig. 2b).

The result of flow cytometric analysis showed that APCA can cause G₂/M phase arrest and G₂/M phase accumulation peaked at 24 h treatment, and subsequently the sub-G₁ phase increased obviously after more than 24 h treatment (Fig. 6), suggesting the sequential events of cell cycle arrest followed by apoptosis. Besides the increase of sub-G₁ cells, apoptosis was confirmed by characteristic morphological changes. The morphological changes of apoptosis include membrane blebbing, cell shrinkage, chromatin condensation, and formation of apoptotic bodies [21]. Staining with Hoechst 33258 clearly showed condensed and fragmented nuclei and apoptotic bodies in the treated cells (Fig. 4).

Cell cycle dysregulation is a hallmark of tumor cells. Regulation of proteins that mediate critical events of the cell cycle may be a useful antitumor target [22]. The cell cycle is mediated by the activation of a highly conserved family of protein kinases, the Cdk1 [22,23]. A number of Cdk1s have been isolated and shown to regulate the cell cycle event in mammalian cells [24]. Activation of Cdk1 requires binding to a specific regulatory subunit, termed a cyclin. Together, these cyclin/Cdk complexes are the cell cycle regulators. The entry into mitosis is under the control of B-type cyclins, which also associate with Cdk1; the cyclinB1/Cdk1 complex is the primary regulator of transition from G₂ to M phase [25]. The cyclinB1/Cdk1 complex was originally defined as the maturation-promoting factor or M phase-promoting factor [26,27]. Regulation of cyclinB1/Cdk1 complexes at multiple levels ensures the tight control of the timing of mitotic entry and cell division. Without synthesis of cyclinB1 before the

G₂/M transition, Cdk1 remains inactive, and the cell cannot enter mitosis; the cell cycle will arrest at G₂ phase. In this study, we found that Cdk1 and cyclinB1 proteins were decreased in a dose-dependent manner after treatment with APCA (Fig. 8), suggesting that APCA could arrest HeLa cells in G₂/M phase. Western blotting analysis and semiquantitative RT-PCR assay demonstrated that the cyclinB1 and Cdk1 were decreased by

Fig. 9



Effect of 3-(dimethylamino-ethylamino)-8-oxo-8H-acenaphthol [1,2-b] pyrrole-9-carboxylic acid (APCA) on mRNA expression of cyclin-dependent kinase 1 (Cdk1), cyclinB1, cyclin D1, CDK4, p53, and p21 in HeLa cells. Cells were treated with APCA (0, 7.5, 15, and 30 μ mol/l) for 24 h and then harvested. The total RNA was extracted, then cDNA was synthesized from total RNA (2 μ g), which was amplified using the sets of primers for examining the expression of Cdk1, cyclinB1, cyclin D1, CDK4, p53, and p21. Quantification of the bands was performed and normalized change folds in relation to untreated cells are shown in parenthesis. Data are presented as mean \pm standard deviation and representative of an average of three independent experiments per concentration. Significant differences from control are indicated by * P <0.05; ** P <0.01; *** P <0.001.

APCA in transcription level and protein level (Figs 8a and 9). This suggested that APCA arrested the cells at the G₂ phase, preventing them from entering mitosis, by decreasing mRNA of cyclinB1 and Cdk1, influencing the expression of cyclinB1 and Cdk1, and then the level of cyclinB1/Cdk1 complex degrades. Thus, our data suggest that cell cycle arrest is mediated by limitation of the supply of Cdk1 and cyclinB1 to the cyclinB1/Cdk1 complex formation, which is an essential step in regulating passage into mitosis.

As a tumor suppressor gene, p53 plays a crucial role in causing cell cycle arrest, apoptosis, and repair. p21, as a cyclin-dependent kinase 2 inhibitor, is also known for its ability to be upregulated by p53, both of which are integrated into G₁ and G₂ arrest machinery in response to DNA damage [28–30]. The common pathway reported was that p53 upregulating p21 resulted in decreasing cyclinB1/Cdk1 complex, and then G₂/M phase arrest occurred [31,32]. This study showed that the expression of p21 and p53 remained unchanged after APCA treatment (Fig. 8b). It was supposed that APCA induced cell cycle arrest and apoptosis without activation of the p53/p21 system. Another pathway reported by Seitz *et al.* [33] was that the nuclear translocation of NF- κ B contributed to the increase of p21 and the following cell cycle arrest. However, our study suggested that the intranuclear amount of NF- κ B was reduced (Fig. 8c). Thus, APCA should arrest cells at the G₂ phase by downregulating the level of cyclinB1 and Cdk1, independently of p53 and NF- κ B.

The inhibition of cell viability observed in APCA-treated cells may also be due to apoptosis (Fig. 6). Cells failing to progress to mitosis may be destined to apoptosis by APCA. Apoptosis is a fundamental process essential for both the development and maintenance of tissue homeostasis and this process was first recognized by Kerr *et al.* [34]. The morphological changes of apoptosis include membrane blebbing, cell shrinkage, chromatin condensation, DNA fragmentation, and formation of apoptotic bodies [35]. We observed that the appearance of the sub-G₁ population after APCA treatment was accompanied by these characteristics for apoptosis morphological changes, as indicated by Hoechst 33258 staining (Fig. 4). Apoptosis has two major pathways: the death-receptor-induced extrinsic pathway and the mitochondria-apoptosome-mediated apoptotic intrinsic pathway [36]. In the mitochondria pathway, NF- κ B is one of the critical transcription factors that regulate the transcription of many genes associated with tumorigenesis. Bcl-2 family proteins also have a central role in controlling the mitochondrial pathway. In humans, more than 20 members of this family have been identified including proteins that suppress apoptosis (e.g. Bcl-2, Bcl-x1, Bcl-1) and proteins that promote apoptosis (e.g. Bax, Bak, Bad) [37]. The proapoptotic proteins and antiapoptotic proteins of the Bcl-2 family may turn apoptosis on and off because of the formation of heterodimers among these

proteins [38–40]. The heterodimerization results in mutual neutralization of the bound proapoptotic and antiapoptotic proteins. Therefore, the balance between the expression levels of the protein units (e.g. Bcl-2 and Bax) is critical for cell survival or death. The result showed that APCA suppressed NF- κ B nuclear localization, which led to upregulation of the Bax level and concomitantly downregulation of Bcl-2 level (Fig. 8d), and then cell apoptosis occurred. Moreover, studies [41] indicated that the augmentation in the Bcl-2/Bax ratio might contribute to apoptosis through caspase activation in the mitochondria pathway.

We also determined the caspase activation and PARP cleavage. The caspases, a family of cysteine proteases, were activated in a cascade of sequential cleavage reaction from their inactive zymogen precursors. Caspase-3 is an executioner caspase, which upon activation can systematically dismantle cells by cleaving key proteins such as PARP. Activation of caspase-3 was observed in APCA-treated cells (Fig. 7). Caspase-3 is an executioner caspase that can be activated by a mitochondrial pathway involving caspase-9 or a death receptor pathway involving caspase-8 [42]. In this study, APCA treatment caused activation of caspase-9 but not caspase-8 (Fig. 7) and PARP cleavage. These results suggested involvement of mitochondrial death pathways in APCA-induced apoptosis.

In summary, our data indicated that APCA at biologically relevant concentration induced cell cycle arrest in the G₂/M phase and apoptosis of human cervix carcinoma cells in a dose-dependent and time-dependent manner. APCA-induced cell cycle arrest was associated with reduction in the protein and mRNA level of Cdk1 and cyclinB1 in a p53-independent manner. Furthermore, inhibition of NF- κ B nuclear translocation and increase in Bax/Bcl-2 ratios were observed after HeLa cells were treated with APCA, which was accompanied by activated caspase-3 and caspase-9 and PARP cleavage. Taken together, these observations indicated that mitochondria-mediated processes may be involved in the induction of apoptosis of cells treated with APCA. The ability of APCA to induce cell cycle arrest at G₂/M phase followed by very effective induction of apoptosis in HeLa cells gives us an additional argument to consider this compound as a novel, potent, and promising therapeutic agent against cervix carcinoma cancer.

Acknowledgements

This study was supported by the Shanghai Leading Academic Discipline Project, Project no. B507, the National Special Fund for State Key Laboratory of Bioreactor Engineering, grant no. 2060204, the Shanghai Committee of Science and Technology, no. 09JC1404500, and the 111 Project, grant no. B07023.

Conflicts of interest

There are no conflicts of interest.

References

- Torres K, Horwitz SB. Mechanisms of taxol-induced cell death are concentration dependent. *Cancer Res* 1998; **58**:3620–3626.
- Gamet-Payastre L, Li P, Lumeau S, Cassar G, Dupont MA, Chevrolleau S, *et al.* Sulforaphane, a naturally occurring isothiocyanate, induces cell cycle arrest and apoptosis in HT29 human colon cancer cells. *Cancer Res* 2000; **60**:1426–1433.
- King RW, Jackson PK, Kirschner MW. Mitosis in transition. *Cell* 1994; **79**:563–571.
- Lewin B. Driving the cell cycle: M phase kinase, its partners and substrates. *Cell* 1990; **61**:743–752.
- Shi Y. Mechanisms of caspase activation and inhibition during apoptosis. *Mol Cell* 2002; **9**:459–470.
- Xie LJ, Xiao Y, Wang F, Xu YF, Qian XH, Zhang R, *et al.* Novel acenaphtho [1,2-b]pyrrole-carboxylic acid family: synthesis, cytotoxicity, DNA-binding and cell cycle evaluation. *Bioorg Med Chem* 2009; **21**:7615–7762.
- Liu JW, Yang F, Zhang Y, Li JY. Studies on the cell immunosuppressive mechanism of Ordonin from *Isodon serra*. *Int Immunopharmacol* 2007; **7**:945–954.
- Es-Saad D, Simon A, Ollier M, Maurizis JC, Chulia AJ, Delage C. Inhibitory effect of ursolic on B16 proliferation through cell cycle arrest. *Cancer Lett* 1996; **106**:193–197.
- Niu YL, Cao SL, Jiang YY, Du W, Zhao YF. Apoptosis of K562 cell induced by N-phosphoryl dipeptide methyl ester. *Clin J Cancer* 2002; **21**:823–827.
- Wang G, Chen HF, Huang MH, Wang NL, Zhang JC, Zhang YA, *et al.* Methyl protodioscin induces G₂/M cell cycle arrest and apoptosis in HepG2 liver cancer cells. *Cancer Lett* 2006; **241**:102–109.
- Levites Y, Youdim MBH, Maor G, Mandel S. Attenuation of 6-hydroxydopamine (6-OHDA)-induced nuclear factor-kappa B (NF-kappa B) activation and cell death by tea extracts in neuronal cultures. *Biochem Pharmacol* 2002; **63**:21–29.
- Zhang J, Shen YL, Liu JW, Wei DZ. Antimetastatic effect of prodigiosin through inhibition of tumor invasion. *Biochem Pharmacol* 2005; **69**:407–414.
- Brune B, Kneten VA, Sandau KB. Nitric oxide and its role in apoptosis. *Eur J Pharmacol* 1998; **351**:261–272.
- Oliver FJ, De la Rubia G, Rolli V, Ruiz-Ruiz MC, De Murcia G, Murcia JM. Importance of poly-(ADP-ribose) polymerase and its cleavage in apoptosis. *J Biol Chem* 1998; **273**:33533–33539.
- Kaufmann SH, Desnoyers S, Ottaviano Y, Davidson NE, Poirier GG. Specific proteolytic cleavage of poly-(ADP-ribose) polymerase: an early marker of chemotherapy induced apoptosis. *Cancer Res* 1993; **53**:3976–3985.
- Orren DK, Petersen LN, Bohr VA. Persistent DNA damage inhibits S-phase and G₂ progression, and results in apoptosis. *Mol Biol Cell* 1997; **8**:1129–1142.
- Hyun JW, Cheon GJ, Kim HS, Lee YS, Choi EY, Yoon BH, *et al.* Radiation sensitivity depends on OGG1 activity status in human leukemia cell lines. *Free Radic Biol Med* 2002; **32**:212–220.
- Ling YH, Consoli U, Tornos C, Andreeff M, Perez-Soler R. Accumulation of cyclin B1, activation of cyclin B1-dependent kinase and induction of programmed cell death in human epidermoid carcinoma KB cells treated with taxol. *Int J Cancer* 1998; **75**:925–932.
- Lock RB, Ross WE. Inhibition of p34cdc2 kinase activity by etoposide or irradiation as a mechanism of G₂ arrest in Chinese hamster ovary cells. *Cancer Res* 1990; **50**:3761–3766.
- Mukherjee AK, Basu S, Sarkar N, Ghosh. AC. Advances in cancer therapy with plant-based natural products. *Curr Med Chem* 2001; **8**:1467–1486.
- Rello S, Stockert JC, Moreno V, Gamez A, Pacheco M, Inarranz A, *et al.* Morphological criteria to distinguish cell death induced by apoptotic and necrotic treatments. *Apoptosis* 2005; **10**:201–208.
- Stewart ZA, Westfall MD, Pietenpol JA. Cell-cycle dysregulation and anticancer therapy. *Trends Pharmacol Sci* 2003; **24**:139–145.
- Sherr CJ. The Pezcoller lecture: cancer cell cycles revisited. *Cancer Res* 2000; **60**:3689–3695.
- Molinari M. Cell cycle checkpoints and their inactivation in human cancer. *Cell Prolif* 2000; **33**:261–274.
- Doree M, Galas S. The cyclin-dependent protein kinases and the control of cell division. *FASEB J* 1994; **8**:1114–1121.
- Smits VAJ, Medema RH. Checking out the G₂/M transition. *Biochim Biophys Acta* 2001; **1519**:1–12.
- O'Connell MJ, Walworth NC, Carr AM. The G₂-phase DNA-damage checkpoint. *Trends Cell Biol* 2000; **10**:296–303.
- Andreassen PR, Lacroix FB, Lohez OD, Margolis RL. Neither p21WAF1 nor 14-3-3s prevents G₂ progression to mitotic catastrophe in human colon carcinoma cells after DNA damage, but p21WAF1 induces stable G₁ arrest in resulting tetraploid cells. *Cancer Res* 2001; **61**:7660–7668.
- El-Deiry WS, Tokino T, Velculescu VE, Levy DB, Parsons R, Trent JM, *et al.* p21 WAF1, a potential mediator of p53 tumor suppression. *Cell* 1993; **75**:817–825.
- El-Deiry WS, Harper JW, O'Connor PM, Velculescu VE, Canman CE, Jackman J, *et al.* WAF1/CIP1 is induced in p53-mediated G₁ arrest and apoptosis. *Cancer Res* 1994; **54**:1169–1174.
- Haupt S, Berger M, Goldberg Z, Haupt Y. Apoptosis – the p53 network. *J Cell Sci* 2003; **116**:4077–4085.
- Innocente SA, Abrahamson JLA, Cogswell JP, Lee JM. p53 regulates a G₂ checkpoint through Cyclin B1. *Proc Natl Acad Sci USA* 1999; **96**:2147–2152.
- Seitz CS, Deng H, Khavari PA. NK-κB triggers cell cycle arrest in epidermis via specific induction of the cyclin dependent kinase inhibitor p21Cip1. *J Dermatol Sci* 1998; **16**:3.
- Kerr JF, Wyllie AH, Currie AR. Apoptosis: a basic biological phenomenon with wide-ranging implications in tissue kinetics. *Br J Cancer* 1972; **26**:239–257.
- Rello S, Stockert JC, Moreno V, Gamez A, Pacheco M, Juarranz A, *et al.* Morphological criteria to distinguish cell death induced by apoptotic and necrotic treatments. *Apoptosis* 2005; **10**:201–208.
- Hu W, Kavanagh JJ. Anticancer therapy targeting the apoptotic pathway. *Lancet Oncol* 2003; **4**:721–729.
- Adams JM, Cory S. The Bcl-2 protein family: arbiters of cell survival. *Science* 1998; **281**:1322–1326.
- Andrew M. Cyclin ubiquitination: the destructive end of mitosis. *Cell* 1995; **81**:149–152.
- Antonsson B, Martinou JC. The Bcl-2 protein family. *Exp Cell Res* 2000; **256**:50–57.
- Reed JC. Double identity for proteins of the Bcl-2 family. *Nature* 1997; **387**:773–776.
- Cohen GM. Caspases: the executioners of apoptosis. *Biochem J* 1997; **326**:1–16.
- Ashkenazi A, Dixit VM. Death receptor: signaling and modulation. *Science* 1998; **281**:1305–1308.